



Research Article








Received: January 14, 2025

Accepted: January 28, 2025

Published: February 5, 2025

ISSN 2304-6295

# Vibration characteristics of 3D curved cellular bridges via panel element method

Temimi, Feras AbdulRidha AbdulRazzaq<sup>1,2</sup>    
 Ahmed, Ahmed Ramadan<sup>1</sup>    
 Obaidi, Amenah Hasan Felaih<sup>2</sup>    
 Yermoshin, Nikolay Alekseevich<sup>1</sup> 

<sup>1</sup> Peter the Great St. Petersburg Polytechnic University, St. Petersburg, Russian Federation; [feras.temimi@utq.edu.iq](mailto:feras.temimi@utq.edu.iq) (T.F.A.A.), [engahmedramadan103@gmail.com](mailto:engahmedramadan103@gmail.com) (A.A.R.), [ermonata@mail.ru](mailto:ermonata@mail.ru) (Y.N.A.)

<sup>2</sup> University of Thi-Qar, Thi-Qar, Iraq; [amnah.h@utq.edu.iq](mailto:amnah.h@utq.edu.iq) (O.A.H.F.)

Correspondence: \* email [altemimi.f@edu.spbstu.ru](mailto:altemimi.f@edu.spbstu.ru); contact phone [+79523734133](tel:+79523734133)

## Keywords:

Panel Element Method (PEM); Finite Element Method (FEM); Structural Dynamics; Free Vibration Analysis; Curved Cellular Bridges; Natural Frequencies; Mode Shapes

## Abstract:

**The object of research** is the development of a novel approach for the free vibration analysis of 3D curved cellular bridges using the Panel Element Method (PEM). The free vibration analysis of 3D curved cellular bridges was performed by the proposed Panel Element Method (PEM). The objective of this research is to examine the relationship between natural frequencies, mode shapes, and computational efficiency and the geometric configuration of curved bridge decks. **Method.** The PEM simulates curved cellular decks as assemblies of planar and non-planar panel modules based on a wide column analogy where two rigid arms joined by a flexible member mimic coupling between bending and torsion. Intrinsic dynamic properties are determined analytically using strain energy minimum principles, implemented in MATLAB for parametric analysis. Comparison with the Finite Element Method (FEM) assesses mode of vibration discrepancies and computational cost. Validation is done externally by solving the equations of equilibrium for bridge geometries with different curvature radius, support types, and cell shapes. **Results.** The PEM is verified against FEM by a variety of case studies for various bridge profiles and supports. It is found that the natural frequencies and mode shapes could be predicted accurately by the PEM with variation of less than 7% in fundamental modes compared to FEM. A high degree of computational efficiency by PEM is proved with over 90% savings in computational efforts without any accuracy loss. The paper concludes that the PEM is a good method for free vibration analysis that can achieve a compromise between accuracy and computational efficiency and is a possible substitute for the analysis of the dynamic behavior of curved bridge decks with various configurations.

## 1 Introduction

The dynamic analysis of three-dimensional curved cellular structures has become one of the important and interesting areas of research in modern engineering, which is favored by their gradual popularity in urban structures. The mathematical formulation of these more-than-elaborate systems, constructed in the original form to cross the vast distances over which traffic flows, was the first step whereas today they are systematically used for the analysis of other designs by machines and computers. However, aside from the fact that these structures include an intricate network of interacting elements, the extreme case of the non-linear inter-relationships of the geometric function of these structures, which makes prediction of the behavior of their vibration under dynamic loading very complicated, the use of advanced computational methods is necessary. Further, the extreme visibility of

Temimi, F.A.A.; Ahmed, A.R.; Obaidi, A.H.F.; Yermoshin, N.

Vibration characteristics of 3D curved cellular bridges via panel element method

2025; Construction of Unique Buildings and Structures; **116** Article No 11601. doi: 10.4123/CUBS.116.1



the geometric features of such structures in the deck-movement of the tubes spanning the bridge's wings—such as mechanical types of monoclomb and the interactions of numerous substituted parts, which are interrelated among the above bandwidth, made it extraordinarily complex to predict the vibration response of the structure during its natural and forced executions [1].

Vibration characteristics of structures, including those curved, are one of the widely studied topics. Huffington and Hoppmann (2021) used the modal Eigen-functions of orthotropic plates to compute the frequencies and eigenfunctions of the structures forming the basis of this work [2]. Cheung et al. (1971) applied the Finite Strip Method to the analyses of bridges of any size and thickness [3]. Bickford and Strom (1975) used the transfer matrix for the analysis of curved beams [4]. Al-Khazraji, et al. (2010) put forward the bilevel calculus to specializing both the straight and curved cellular bridges, in turn, upon which this research was to be based [5]. Agarwal P. et al. (2022) employed a finite element method to examine free vibration in 420 varied parameters models of the box-girder type bridge [6]. Nidhi Gupta, et al. (2019) used the finite element method on the solver SAP2000 to analyze the vibration frequencies of the simply supported and RCC box-girder bridge with a varying curvature in the numerical experiment [7].

Traditional approaches, such as the Finite Element Method (FEM), remain widely employed for free vibration analysis. Studies by Verma and Nallasivam (2023) and Xiang et al. (2023) demonstrate FEM's utility in modeling vehicle-bridge interactions and stochastic resonance effects in curved box girders [8], [9]. Similarly, Zhu et al. (2023) applied the Extended Finite Element Method (XFEM) to analyze crack propagation in bridge decks [10], while Ahmad et al. (2023) explored damage impacts on vibrational characteristics via nonlinear FEM [11]. Despite its versatility, FEM faces limitations in computational efficiency and accuracy for curved cellular systems, particularly under multi-component loading scenarios [12], [13].

There have been recent developments in computational techniques that have greatly improved the capability to analyze the dynamic response of intricate structures. Traditional methods, such as the Finite Element Method (FEM), have been widely employed for free vibration analysis. However, FEM can be computationally intensive, especially for intricate geometries like 3D curved cellular bridges, necessitating the exploration of alternative approaches that balance accuracy and computational efficiency. The Panel Element Method (PEM) has emerged as a promising alternative, simplifying the modeling of curved cellular bridge decks by representing them as assemblages of planar and non-planar panel units. This approach not only reduces the degrees of freedom but also maintains a high level of accuracy in predicting natural frequencies and mode shapes [14] – [16].

Novel methods like the Panel Element Method (PEM) offer a promising alternative. By dividing curved decks into planar and non-planar panel units, PEM achieves ease of modeling at no cost in geometric accuracy [17]. Al\_Temimi (2014) further highlight PEM's potential to enhance computational efficiency [17]. Nevertheless, comprehensive validation of PEM against FEM for curved cellular bridges remains sparse. For instance, studies by some researchers have identified gaps in PEM's application to dynamic load predictions, particularly for systems involving train-track-bridge interactions [18] or pedestrian-induced vibrations [19].

Complementary research underscores additional challenges. Verma et al. (2025) developed regression models to predict dynamic responses of thin-walled girders [20], while Zhang et al. (2020) proposed frequency-domain frameworks to reduce computational costs [21]. Consolazio et al. (2004) emphasized the role of dynamic load modeling in pier impacts [22], and Owerko (2018) highlighted unresolved methodological limitations in PEM validation [23]. These works collectively reveal a pressing need for systematic comparisons between PEM and FEM to establish robust predictive frameworks [24].

This study addresses these gaps by evaluating PEM's efficacy in analyzing free vibrations of three-dimensional curved cellular bridges. Through parametric comparisons with FEM, the research assesses PEM's computational efficiency, accuracy in modal frequency prediction, and applicability to diverse loading scenarios—including stochastic, vehicular, and pedestrian-induced vibrations. By integrating insights from structural integrity [10], damage modeling [11], and load detection algorithms [13], the work aims to refine PEM's utility for optimizing the seismic and dynamic design of modern bridges.

The primary aim of this study was to study the free vibration analysis of three-dimensional curved cellular bridges, especially their dynamic behavior and vibrational characteristics. The new computational methods, specifically the Panel Element Method (PEM), were used in this research to enhance the accuracy and effectiveness of vibration analysis. The objective was to provide a unique understanding of the vibrational response of curved cellular bridges to different loads thus contributing to the design and

safety of these vital infrastructures. The tasks involved examining how effective PEM is, to compare it with the classical methods, and to determine its applicability to different bridge types.

The methodical nature of this study is intended to bridge the existing gaps in scholarly knowledge and to provide a basis for advancing knowledge in the field of seismic and dynamic analysis and design of road bridges.

## 2 Materials and Methods

### 2.1 Description of the panel element method (PEM)

An idealization procedure for the panel element (PE), termed the Panel Element Method (PEM), is presented. This analogous frame approach modifies an existing frame method element. The proposed PE and PEM serve as idealization for modeling curved cellular bridge decks.

### 2.2 Basis and Assumptions of the Panel Element (PE)

The proposed panel element, based on the Wide Column Analogy [17] shown in (Fig. 1a), consists of two horizontal rigid arms connected by a central flexible beam. Each element has four nodes, with three translational and one rotational degree of freedom per node, see (Fig. 1c). The rigid arms constrain in-plane translations and out-of-plane rotations to be identical, resulting in twelve degrees of freedom per element, as shown in (Fig. 1d).

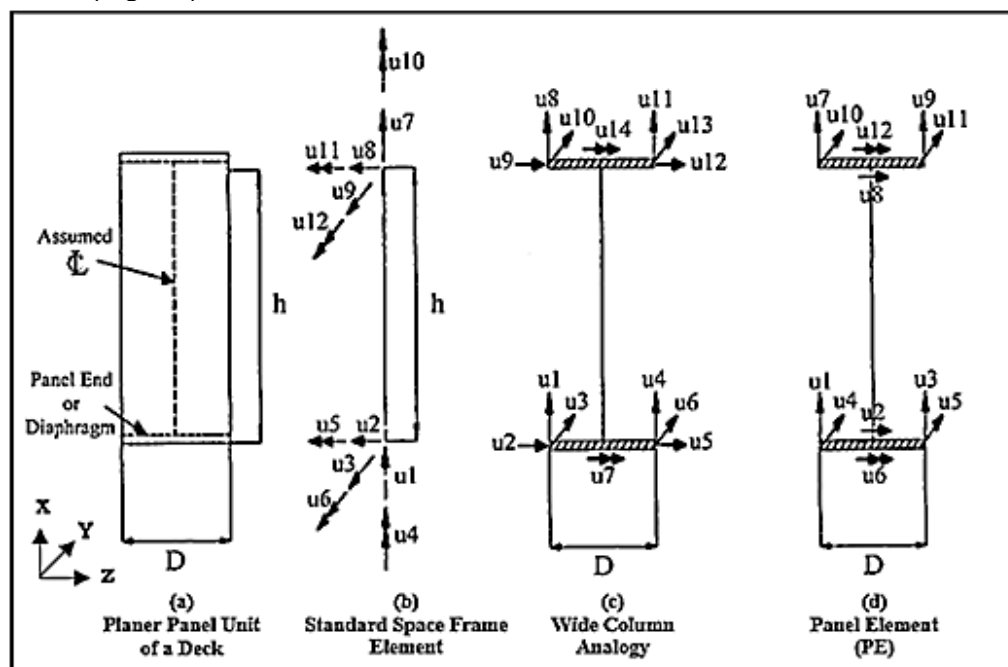


Fig. 1 - Development of the Panel Element (PE) [17]

The derivation and modification of the Panel Element Method (PEM) are based on these assumptions:

1. The bridge is modeled as a finite assemblage of flat plates or wall panels.
2. Each panel is represented by a conventional space frame element.
3. In-plane flexural and shear deformations of each panel element (PE) are included.
4. Out-of-plane flexural and shear deformations of each PE are also included.
5. Diaphragms are infinitely rigid in-planes and flexible out-of-planes.

### 2.3 Stiffness Matrix of the Panel Element

The element stiffness matrix  $[K_e]$  for the in-plane and out-of-plane degrees of freedom is derived from the standard space frame element stiffness matrix  $[K_c]$  (Fig. 1b) [17], as the degrees of freedom are kinematically relateable, such that:

$$\{u_c\} = [T_e] \cdot \{u_e\} \quad (1)$$



Where:  $[T_e]$  - is the transformation matrix, a kinematic transformation, given by:

$$[T_e] = \begin{bmatrix} [T_{e1}] & [0] \\ [0] & [T_{e1}] \end{bmatrix} \quad (2)$$

The sub-matrices  $[T_{e1}]$  are derived using the master-slave transformation concept, connecting the element's degrees of freedom in (Fig. 1d) with the conventional 3-D beam column degrees of freedom in (Fig. 1b) for both in-plane and out-of-plane elements [17].

The stiffness matrix  $[K_e]$  of the panel element is given by Eq. (3), and the stiffness matrix  $[K_c]$  of the standard space frame element (Fig. 1b) can be expressed as below. The sub-matrices of the stiffness matrix  $[K_{ii}]$  and  $[K_{jj}]$  are defined, with lower signs of off-diagonal elements for  $[K_{ii}]$  and upper signs for  $[K_{jj}]$  [17].

$$[K_e] = [T_e]^T \cdot [K_c] \cdot [T_e] \quad (3)$$

$$[K_c] = \begin{bmatrix} [K_{ii}] & [K_{ij}] \\ [K_{ij}]^T & [K_{jj}] \end{bmatrix} \quad (4)$$

## 2.4 Mass Matrix of the Panel Element

The mass matrix of the panel element can be expressed in terms of the space frame unit, as follows:

### 2.4.1 Consistent mass matrix of the panel element

The element mass matrix  $[M_e]$  for the in-plane and out-of-plane degrees of freedom at the panel element nodal points are derived from the mass matrix  $[M_c]$  of the standard space frame element (Fig. 1b) [17], corresponding to the kinematically equivalent degrees of freedom. Thus, the mass matrix  $[M_e]$  is given by Eq. (5), and the mass matrix  $[M_c]$  of the standard space frame element (Fig. 1b) can be expressed as below. The sub-matrices of the mass matrix  $[M_{ii}]$  and  $[M_{jj}]$  are defined, with lower signs of off-diagonal elements for  $[M_{ii}]$  and upper signs for  $[M_{jj}]$  [17].

$$[M_e] = [T_e]^T \cdot [M_c] \cdot [T_e] \quad (5)$$

$$[M_c] = \begin{bmatrix} [M_{ii}] & [M_{ij}] \\ [M_{ij}]^T & [M_{jj}] \end{bmatrix} \quad (6)$$

### 2.4.2 HRZ mass matrix of the panel element

The "HRZ" name refers to the authors of the procedure below. The HRZ Lumping Scheme [25] effectively provides a diagonal mass matrix for arbitrary elements by computing only the diagonal terms of the consistent element mass matrix and scaling them to preserve the total element mass. This results in a diagonal mass matrix, accommodating both translational and rotational degrees of freedom in 1, 2, or 3 directions. The steps are:

1. Compute the diagonal coefficients ( $m_{ii}$ ) of the consistent element mass matrix, ( $m_{11}, m_{22}, \dots, m_{nn}$ ) (Fig. 2).
2. Compute the total mass of the panel element, ( $m_p$ ), equal to:  $m_p = \rho \cdot A \cdot h$
3. Determine ( $S_c$ ) for each coordinate direction by summing diagonal coefficients ( $m_{ii}$ ) associated with translational degrees of freedom, excluding rotational ones, that are parallel and in the same direction.
4. Scale all diagonal coefficients ( $m_{ii}$ ) for this direction by ( $m_p/S_c$ ) to preserve the total mass.
5. Apply these steps to convert the consistent mass matrix to a lumped mass matrix  $[M_l]$ .
6. The panel element mass matrix  $[M_e]$  is given by:

$$[M_e] = [T_e]^T \cdot [M_l] \cdot [T_e] \quad (7)$$

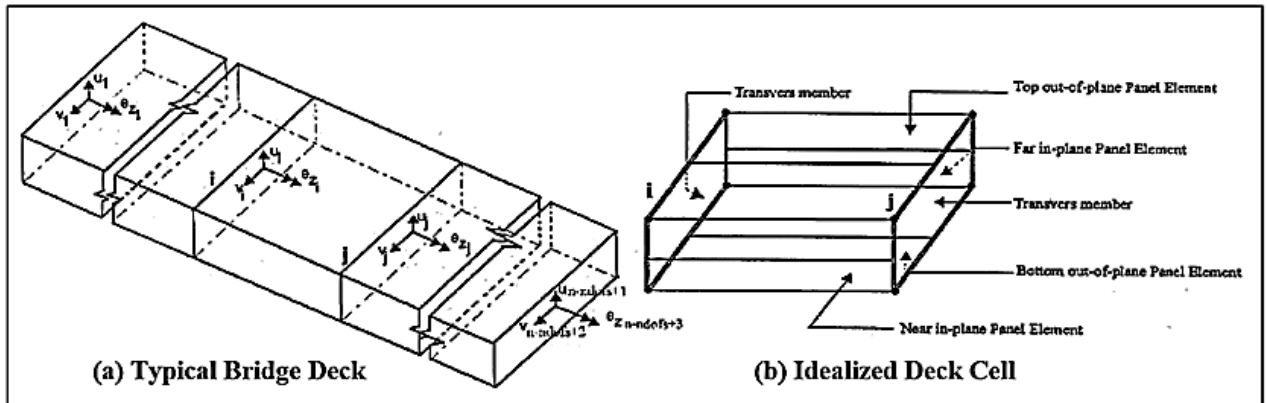


Fig. 2 - Idealization of the Panel Element (PE) [17]

The HRZ lumping technique yields a simple diagonal mass matrix, maintaining the total degrees of freedom of the global structure, and simplifies numerical solutions by reducing storage needs and computation time.

### 2.5 Effect of The Rigid Diaphragms

Rigid diaphragms can be located on the right, left, or either side of panel elements. They are assumed to be infinitely rigid in-planes and flexible out-of-planes. In the Panel Element Method (PEM), units connect via diaphragms on one or both sides. Thus, panel degrees of freedom in the diaphragm plane depend on three in-plane degrees of freedom (two translations, one rotation) of a master node at the bridge cross-section's center of mass [17].

This assumption reduces the dynamic structure's degrees of freedom, assuming no distortion in the cellular curved bridge cross-section, which is reasonable for most such bridges. It implies that with intermediate diaphragms, the cross-section remains undistorted, while translational degrees of freedom along the deck's longitudinal axis are unconstrained, allowing for longitudinal warping during torsional deformation. Consequently, the panel element stiffness  $[K_{me}]$  and mass matrices  $[M_{me}]$  contribute to the structure's property matrices concerning the degrees of freedom of a typical cell panel (Fig. 3), taking the form:

$$[K_{me}] = [T_g]^T \cdot [K_e] \cdot [T_g] \tag{8}$$

$$[M_{me}] = [T_g]^T \cdot [M_e] \cdot [T_g] \tag{9}$$

Here,  $[K_e]$  and  $[M_e]$  are the panel element stiffness and mass matrices from Eq. (3) and Eq. (5) or Eq. (7), respectively.  $[T_g]$  is the transformation matrix within diaphragms, relating individual panel element degrees of freedom to the global structure's degrees of freedom (Fig. 3).  $[T_g]$  is defined for panel elements constrained by rigid diaphragms at both ends, at the left end, at the right end, or with no constraints [17].

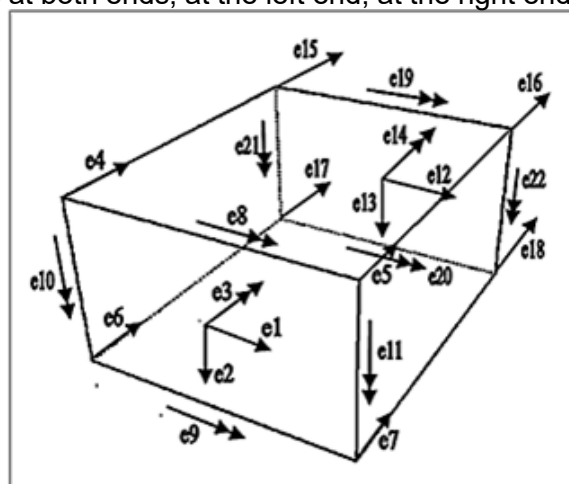


Fig. 3 - Idealization of a Single-Cell Bridge Deck with Rigid Diaphragms Using the Component Element Method

## 2.6 3D-coordinate rotation matrix

Rotation matrices convert between reference systems, crucial for computing joint angles. This section details transforming 3D-coordinate systems, providing a basis for determining global stiffness and mass matrices and developing joint solutions.

The 3D transformation from local to global coordinates is shown in (Fig. 4), where  $(x, y, z)$  is the global system and  $(x_2, y_2, z_2)$  often denoted by  $(\overline{xyz})$ , is the local system.

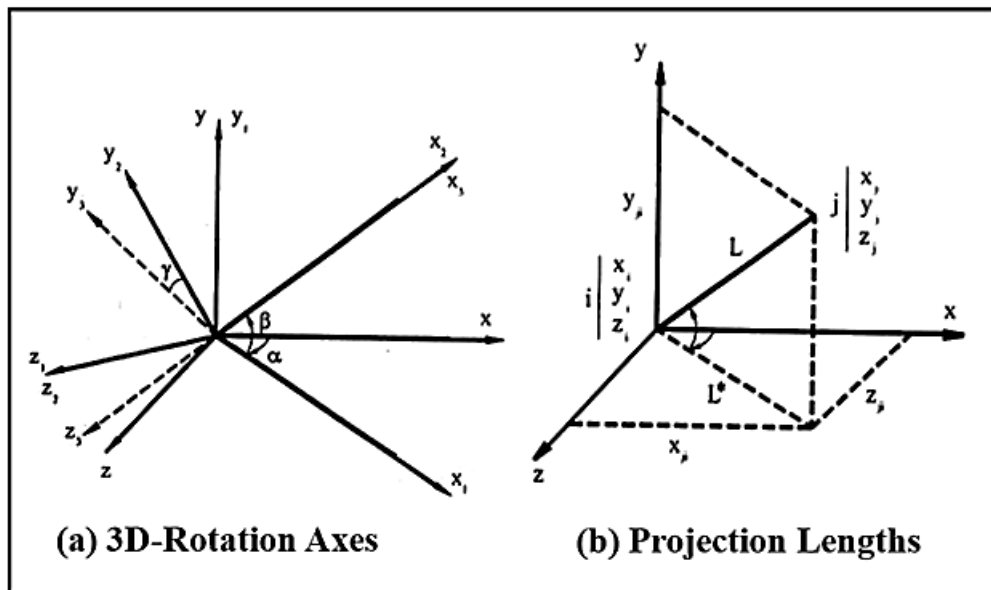


Fig. 4 - Transformation From Local Coordinate System to Global Coordinate System [26]

### 2.6.1 Transformations into System Coordinates

Panel element stiffness and mass matrices refer to local axes  $(x', y', z')$ . Each bridge element may be oriented arbitrarily, requiring transformation to global degrees of freedom before assembling the system matrices. The global axes  $(X, Y, Z)$  align with local axes  $(x', y', z')$  through rotations about  $(Y, X, Z)$  axes, (Fig. 5) [27].

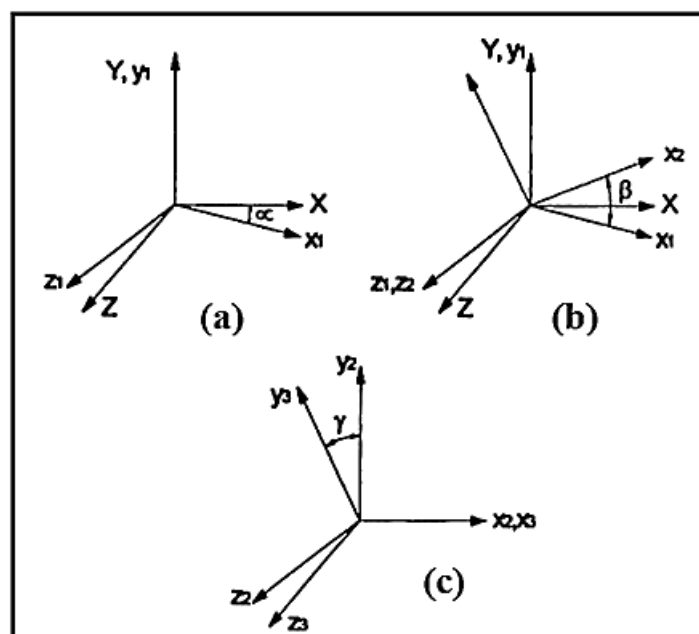


Fig. 5 - Rotation Transformation of Axes for 3-D System [27]

### 2.6.2 Local to Global System Conversion

Element coordinates relate to global coordinates by: [17]

$$\{U_l\} = [T_R] \cdot \{u\} \tag{10}$$

Where:  $\{U\}$ - is the displacement vector in element coordinates,  $[T_R]$ - is the 3D transformation matrix, and  $\{u\}$ - is the displacement vector in global coordinates.

The 3D transformation matrix  $[T_R]$  converts panel element stiffness and mass matrices from local to global coordinates (Eq. 11). The 3D rotation matrix  $[T]$  is a (3x3) transformation matrix as described in (Eq. 12) [17].

$$[T_R] = \begin{bmatrix} [T] & 0 & 0 & 0 \\ 0 & [T] & 0 & 0 \\ 0 & 0 & [T] & 0 \\ 0 & 0 & 0 & [T] \end{bmatrix} \tag{11}$$

$$[T] = \begin{bmatrix} C_1C_2 & S_1C_2 & S_2 \\ (-C_1S_2S_3 - S_1C_3) & (-S_1S_2S_3 + C_1C_3) & S_3C_2 \\ (-C_1S_2C_3 - S_1S_3) & (-S_1S_2S_3 - C_1S_3) & C_3C_2 \end{bmatrix} \tag{12}$$

### 2.6.3 Global Stiffness and Mass Matrices

The global stiffness  $[K_{Ge}]$  and mass  $[M_{Ge}]$  matrices of the panel element, considering the 3D-rotation system conversion, are:

$$[K_{Ge}] = [T_R]^T \cdot [K_{me}] \cdot [T_R] \tag{13}$$

$$[M_{Ge}] = [T_R]^T \cdot [M_{me}] \cdot [T_R] \tag{14}$$

## 2.7 Cellular bridge idealization using (cem)

The global degrees of freedom  $[U]$  for a typical cellular bridge deck system (Fig. 2, Fig. 3, and Fig. 6) using the Component Element Method (CEM) are:

$$\{U\} = \{u \quad v \quad w \quad \theta_z \quad \theta_L\} \tag{15}$$

Where:  $u, v, w$ - are translational displacements in X, Y, Z directions;  $\theta_z$  - is rotational displacement about the Z axis;  $\theta_L$  - is local rotational displacement about each panel element's minor axis.

Thus, the component element stiffness  $[K_{CG}]$  and mass matrices  $[M_{CG}]$  are obtained as follows.

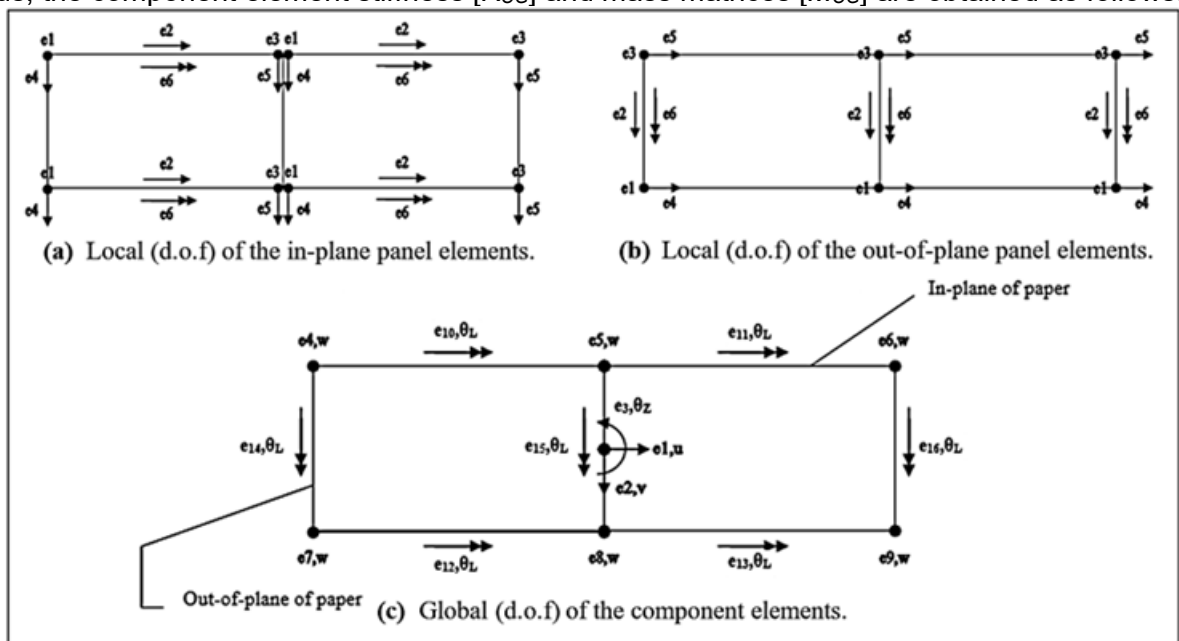


Fig. 6 - Idealization of Double Cellular Bridge by Using Component Element Method (CEM)

### 2.7.1 Component Stiffness and Mass Matrices

The global stiffness  $[K_{CG}]$  and mass  $[M_{CG}]$  matrices of the component element, after assembling all panel element matrices (Fig. 3), are:

$$[K_{CG}] = \begin{bmatrix} K_{uu} & 0 & K_{uw} & 0 & K_{u\theta_L} \\ & K_{vv} & K_{vw} & K_{v\theta_z} & K_{v\theta_L} \\ & & K_{ww} & 0 & 0 \\ & Sym. & & K_{\theta_z\theta_z} & 0 \\ & & & & K_{\theta_L\theta_L} \end{bmatrix} \quad (16)$$

$$[M_{CG}] = \begin{bmatrix} M_{uu} & 0 & M_{uw} & 0 & M_{u\theta_L} \\ & M_{vv} & M_{vw} & M_{v\theta_z} & M_{v\theta_L} \\ & & M_{ww} & 0 & 0 \\ & Sym. & & M_{\theta_z\theta_z} & 0 \\ & & & & M_{\theta_L\theta_L} \end{bmatrix} \quad (17)$$

In Eq. (16) and Eq. (17), sub-matrices  $K_{uu}$ ,  $K_{vv}$ ,  $K_{\theta_z\theta_z}$ ,  $M_{uu}$ ,  $M_{vv}$  and  $M_{\theta_z\theta_z}$  are of order  $(np)$ , where  $(np)$  is the number of panels between diaphragms.

Sub-matrices  $K_{ww}$  and  $M_{ww}$  are of order  $(np \times mp)$ , with  $(mp)$  being the number of longitudinal displacements at each diaphragm, equal to the number of nodes there.  $K_{\theta_L\theta_L}$  and  $M_{\theta_L\theta_L}$  are of order  $(qp \times np)$ , where  $(qp)$  is the number of panel elements forming the curved cellular-bridge deck system.

## 2.8 Finite element idealization method (FEM)

The finite element idealization validates the proposed Panel Element Method (PEM) and serves for comparison. Analyses use ANSYS12 with Beam and Shell 63 (elastic shell) elements.

A cellular bridge deck, comprising top and bottom slabs, vertical webs, and transverse members (rigid diaphragms), is modeled using beam and four-node flat shell elements (Fig. 7, and Fig. 8). For free vibration and earthquake response analysis, mesh size is refined until a maximum difference of less than 2% is achieved in successive solutions.

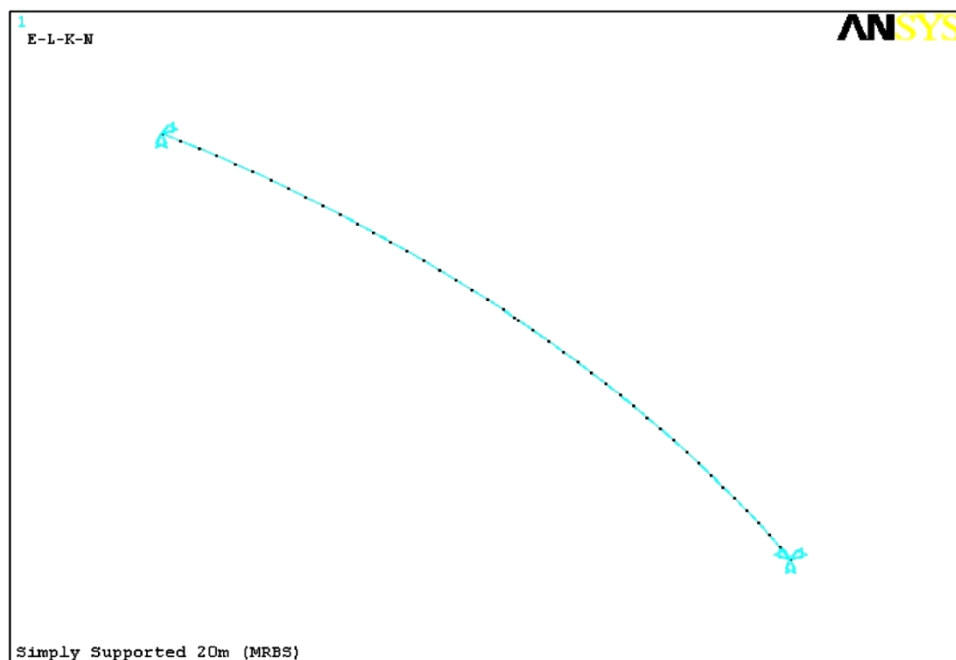
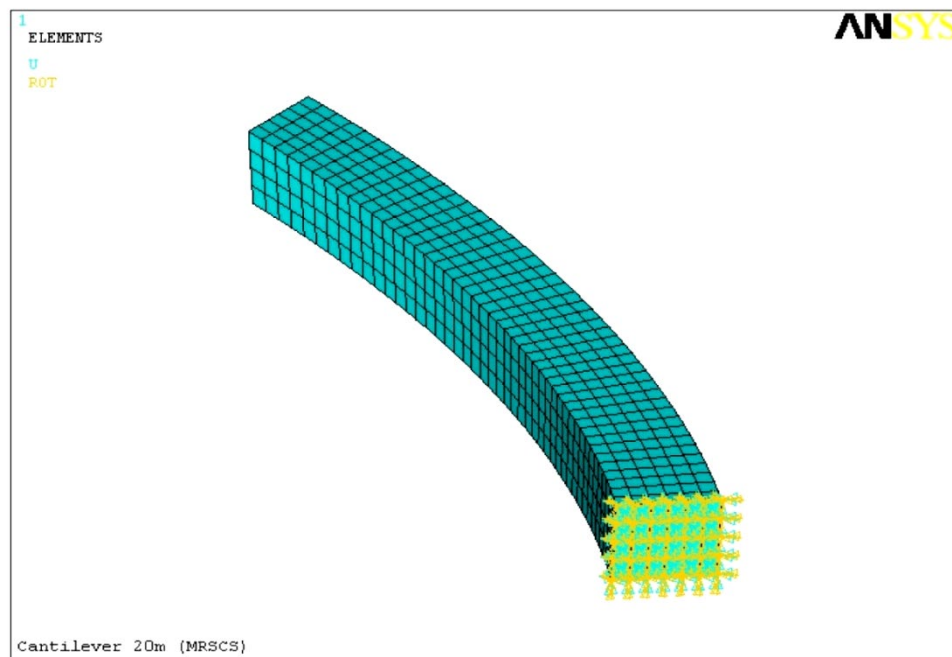


Fig. 7 - Rectangular Single Cell Simply Supported Curved Box Beam Model



**Fig. 8 - Rectangular Single Cell Cantilevers Curved Box Shell Model**

## 2.9 Undamped free vibration analysis

The governing equation of motion for the damped systems is [28]:

$$[M] \cdot \{\ddot{U}\} + [C] \cdot \{\dot{U}\} + [K] \cdot \{U\} = \{F(t)\}, \quad (18)$$

Where:  $\{\ddot{U}\}$ ,  $\{\dot{U}\}$  and  $\{U\}$ - are the time-dependent acceleration, velocity, and displacement vectors.  $[K]$ ,  $[C]$  and  $[M]$ - are global stiffness, damping, and mass matrices.  $\{F(t)\}$ - is the applied load vector.

Assuming classical damping, the damping matrix is:

$$C = 2\zeta_i \cdot \omega_i \cdot M. \quad (19)$$

The governing equation for an undamped free vibration system is derived by removing the damping matrix and load vector from Eq. (18). Assuming the system's free vibration is harmonic, it is expressed as Eq. (21):

$$[M] \cdot \{\ddot{U}\} + [K] \cdot \{U\} = \{0\}, \quad (20)$$

$$\{U(t)\} = \{\hat{U}\} \cdot \sin(\omega_i \cdot t + \hat{\theta}), \quad (21)$$

This equation becomes:

$$U = \Phi \cdot \sin(\omega \cdot t), \quad (22)$$

Substituting  $(U)$  and  $(\ddot{U})$  from Eq. (22) into Eq. (20) gives:

$$K \cdot \Phi = \omega^2 \cdot M \cdot \Phi \quad \text{or} \quad K \cdot \Phi = \lambda \cdot M \cdot \Phi, \quad (23)$$

Where:  $\zeta_i$  - is the damping ratio for mode  $(i)$ ,  $\omega_i$  - is the natural angular velocity for mode  $(i)$ ,  $\hat{U}$  - is the mode shape,  $\hat{\theta}$  - is the phase angle,  $\{0\}$ - is a zero vector,  $\Phi$ - is the eigenvector,  $\omega$ - is the natural frequency, and  $\lambda$ - is the vector of Eigen values, equal to the squares of the natural frequencies vector  $(\omega)$ .

Equations (9) and (10) derive the system's frequency equation [17]:

$$[[K] - \omega_i^2 \cdot [M]] = 0. \tag{24}$$

Expanding this gives an algebraic equation of ( $n^{th}$ ) degree, the characteristic equation [29]. The ( $n$ ) roots, ( $\omega_1^2, \omega_2^2, \omega_3^2, \dots, \omega_n^2$ ), represent the square of the circular frequencies (Eigen values) for ( $n$ ) vibration modes, with corresponding ( $n$ ) eigenvectors as mode shapes. Eq. (24) is solved using MATLAB.

### 2.10 Restriction of support

For simply supported, single-span bridge decks with partial restraint, the Panel Element Method (PEM) is as effective as the Finite Element Method (FEM).

Bridge deck support conditions are:

1. Partially restrained: The end diaphragm is partially restrained out-of-plane, restricting only basic node degrees of freedom (Fig. 9a).
2. Fully restrained: The end diaphragm is fully restrained out-of-plane, restricting all longitudinal degrees of freedom (Fig. 9b).

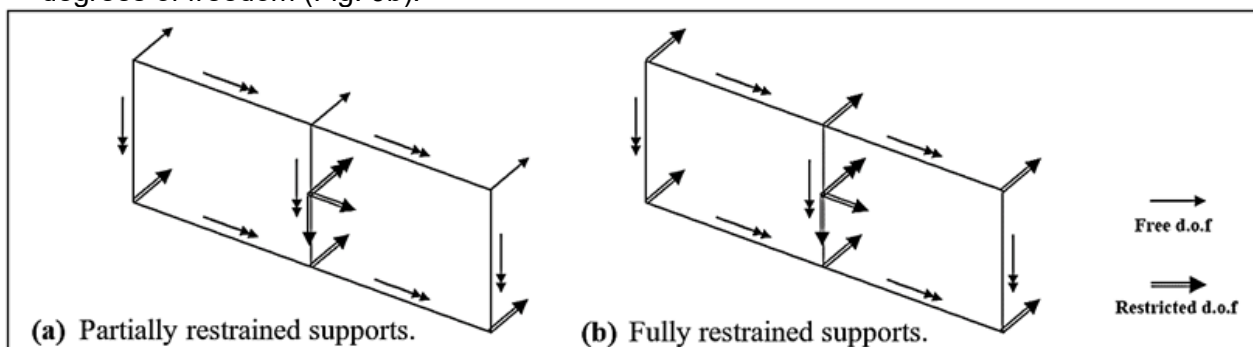


Fig. 9 - Types of Supports Restrained Conditions

### 2.11 Validation case studies

This study examines a single cell curved bridge deck. The layout and dimensions are shown in (Fig. 10). Free vibration analysis of a single-span bridge deck is conducted. The decks are assumed to be reinforced concrete, modeled as linearly elastic and isotropic, with properties listed in (Table 1).

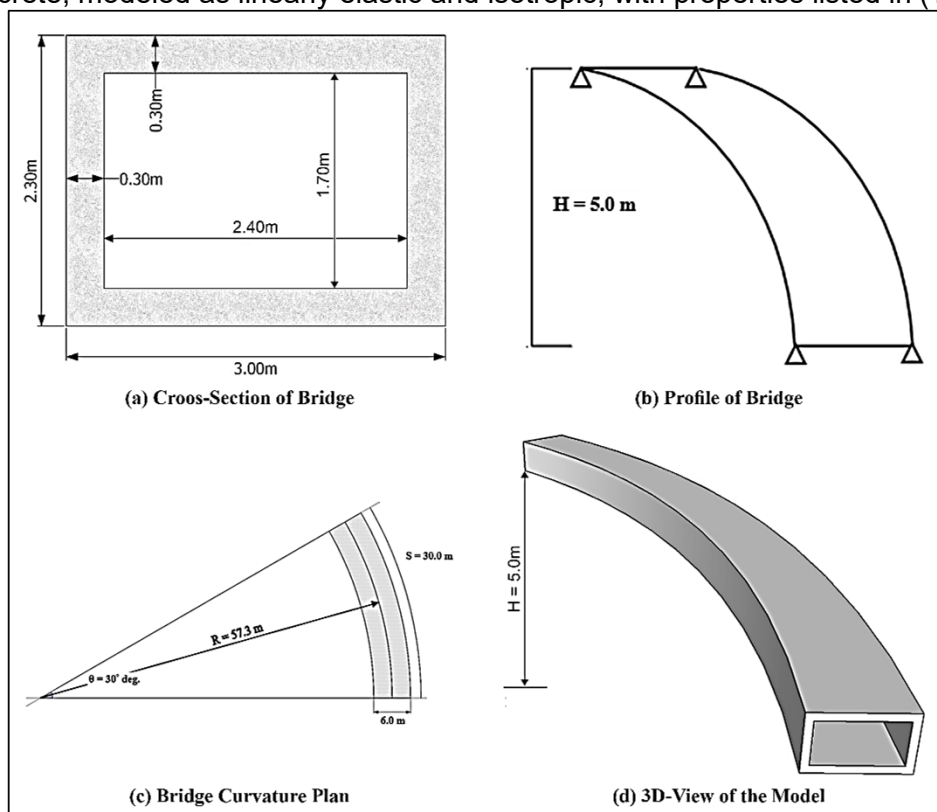


Fig. 10 - Details of Curved Bridge with Single-Cell Cross-Section

Table 1. Material Properties of The Study Cases

No.	Material Properties	Values
1	Elastic Modulus (E)	$23.5 \times 10^6$ kN/m <sup>2</sup>
2	Weight Density ( $\gamma$ )	24.517 kN/m <sup>3</sup>
3	Poisson's Ratio ( $\nu$ )	0.20

For comparison, all decks were modeled using panel elements with twelve (12) degrees of freedom (d.o.f), sufficient to capture the bridge deck's free vibration characteristics. In contrast, the same single-cell and double-cell decks required more elements and degrees of freedom when modeled using the Finite Element Method (FEM) in ANSYS to predict global free vibration characteristics.

Natural frequencies and corresponding mode shapes, derived from the equation of motion in Eq. (20), were evaluated using the inverse iteration scheme. The mass matrix for the first case study was based solely on the deck's weight, while the second case study included live load effects by assuming equivalent lumped masses at live load positions.

### 3 Results and Discussion

#### 3.1 Study verification

Four study verifications were performed on various bridge deck configurations to highlight the accuracy and reliability of the proposed optimization procedure (Panel Element Method (PEM)) to evaluate the behavior of cellular decks in comparison to the Finite Element Method (FEM). The analysis focused on four key aspects: the effect of cell number variation, span length variation, web-to-slab thickness ratio, and the number of diaphragms relative to span length.

##### 3.1.1 Effect of Cell Number Variation

The study demonstrated that the PEM significantly reduces the degree of freedom (d.o.f) required for analysis compared to FEM, particularly in fine mesh scenarios as shown in (Table 2). For instance, in a single cell configuration with a fine mesh, FEM required 900 elements and 5.520 d.o.f, whereas PEM maintained only 16 elements and 55 d.o.f. This highlights PEM's efficiency in handling complex geometries with fewer computational resources.

Table 2. Effect of Cell Number Variation: (NOP: No. of Panels = 4,  $t_s = t_w = 0.3$  m,  $L = 20$  m)

No. of Cells	Mesh Size	Finite Element Method (FEM)		Panel Element Method (PEM)	
		No. of Elements	No. of d.o.f	No. of Elements	No. of d.o.f
Single Cell	Coarse	16	120	16	55
	Fine	900	5520		
Double Cell	Coarse	28	180	28	80
	Fine	1728	10290		

##### 3.1.2 Effect of Span Length Variation

Increasing the span length from 20 m to 30 m showed a substantial increase in the computational demand for FEM, while PEM maintained consistent performance with fewer elements and d.o.f. For a 30 m span with a fine mesh, FEM required 1320 elements and 8040 d.o.f, whereas PEM required only 24 elements and 77 d.o.f, demonstrating its computational efficiency, as shown in (Table 3).

Table 3. Effect of Span Length Variation: (NOP = 4; 6,  $t_s = t_w = 0.3$  m,  $L = 20; 30$  m)

Span Length (L)	Mesh Size	Finite Element Method (FEM)		Panel Element Method (PEM)	
		No. of Elements	No. of d.o.f	No. of Elements	No. of d.o.f
20 m	Coarse	16	120	16	55
	Fine	900	5520		
30 m	Coarse	24	168	24	77
	Fine	1320	8040		



### 3.1.3 Effect of (Web : Slab) Thickness Ratio

Across various thickness ratios, PEM consistently required fewer elements and d.o.f compared to FEM as shown in (Table 4). This indicates that PEM is robust in handling variations in structural design without a significant increase in computational complexity, maintaining 16 elements and 55 d.o.f across all tested ratios.

**Table 4. Effect of (Web : Slab) Thickness Ratio: (NOP = 4,  $t_s = 0.2$  m,  $t_w = 0.1, 0.2, 0.3$  and  $0.4$  m,  $L = 20$  m)**

tw/ts Ratio	No. of Cell	Finite Element Method (FEM)		Panel Element Method (PEM)	
		No. of Elements	No. of d.o.f	No. of Elements	No. of d.o.f
0.5	Single Cellular Deck Bridge	16	120	16	55
1		16	120	16	55
1.5		16	120	16	55
2		16	120	16	55

### 3.1.4 Effect of (No. of Diaphragms : Span) Ratio

The analysis of diaphragm configurations showed that PEM could efficiently model complex geometries with fewer elements and d.o.f. as shown in (Table 5). For example, with 10 panels, FEM required 40 elements and 264 d.o.f, while PEM only required 40 elements and 121 d.o.f, further emphasizing its efficiency.

**Table 5. Effect of (No. of Diaphragms : Span) Ratio: (NOP = 2, 4, 6 and 10,  $t_s = t_w = 0.3$  m,  $L = 20$  m)**

No. of Panels	No. of Cell	Finite Element Method (FEM)		Panel Element Method (PEM)	
		No. of Elements	No. of d.o.f	No. of Elements	No. of d.o.f
2	Single Cellular Deck Bridge	8	72	8	33
4		16	120	16	55
6		24	168	24	77
10		40	264	40	121

## 3.2 Parametric studies

Four parametric studies were conducted to examine the behavior of curved box-girder bridges, focusing on the effect of the number of cells, web-to-flange thickness ratios, number of diaphragms and live load magnitudes.

### 3.2.1 Effect of Number of Cells (Rectangular)

The study examines how the number of cells in rectangular cellular bridge decks affects natural frequencies, comparing FEM and PEM. Both single and double cellular configurations were analyzed across five modes. Results in (Table 6) show FEM and PEM frequencies are closely aligned. PEM is slightly higher in the first mode (2.97 Hz vs. 2.915 Hz) and shows a noticeable difference in the third mode (15.44 Hz vs. 14.724 Hz). Generally, PEM predicts higher frequencies, except in the fourth mode (17.82 Hz vs. 18.718 Hz).

**Table 6. Effect of Number of Cells (Rectangular)**

No. of Cells	Analysis Method	Natural Frequency ( $\omega$ ) in ( Hz ) according to Mode Number				
		1	2	3	4	5
Single Cellular	FEM	2.915	3.671	14.724	18.718	21.250
	PEM	2.97	3.71	15.44	17.82	22.32
Double Cellular	FEM	2.987	6.211	14.218	16.826	26.713
	PEM	3.02	6.23	14.56	16.90	27.76

Figures (11 and 12) show the mode shapes of the first five modes of two types of bridge supports (cantilever, simply supported) for the single cell curved bridge deck. The figures show the extent to which the type of support at the two ends of the bridge affects its mode shape.

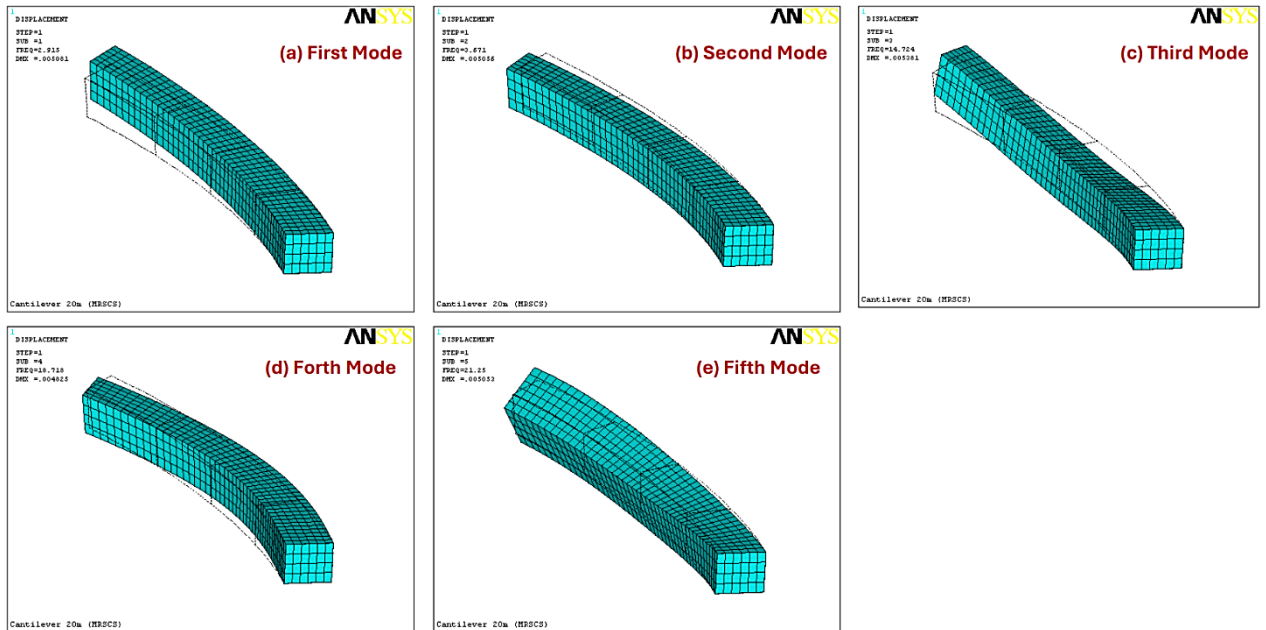


Fig. 11 - Mode Shapes of a Single Cell Cantilever Curved Bridge Deck

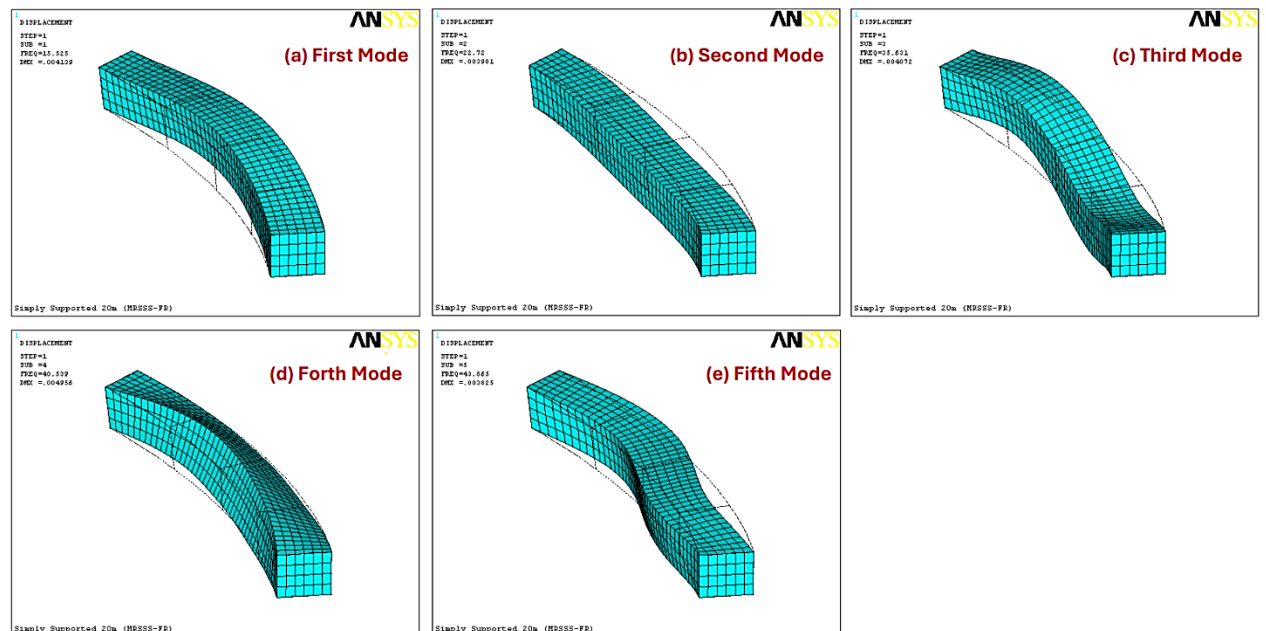


Fig. 12 - Mode Shapes of a Single Cell Simply Supported Curved Bridge Deck (Fully Restrained)

### 3.2.2 Effect Of Web-to-Flange Thicknesses Ratio

A single-cell deck with a depth of 2.3 m and width of 3.0 m was analyzed for a 20 m single span with partially and fully restrained support, and a radius of curvature of 57.3 m. Thickness ratios varied from 0.5 to 2.0. The first five natural frequencies are listed in (Table 7) and (Table 8), with plots in (Fig. 13) and (Fig. 14) for single-cell decks with partially and fully restrained support, respectively.

The study found that increasing the web-to-slab thickness ratio raises the natural frequencies, attributed to enhanced bridge stiffness, particularly in lateral-torsional modes.

Table 7. Natural Frequencies vs. (Web:Slab) Thickness Ratio for a Partially Restrained at Supports

t <sub>w</sub> /t <sub>s</sub> ratio	Analysis Method Type	Natural Frequency (ω) in ( Hz )				
		Mode No. (Single-Cell, Partially Restrained at Supports)				
		1	2	3	4	5
0.5	FEM	7.703	9.045	9.800	10.031	11.662
	PEM	7.78	9.12	10.36	10.43	12.00



1	FEM	10.879	12.785	13.816	13.959	15.245
	PEM	10.93	12.84	14.89	15.05	17.04
1.5	FEM	10.967	14.791	15.292	18.260	19.270
	PEM	11.02	14.86	15.72	19.32	20.48
2	FEM	10.831	16.120	17.209	20.051	21.146
	PEM	10.88	16.19	17.99	20.93	21.91

**Table 8. Natural Frequencies vs. (Web:Slab) Thickness Ratio for a Fully Restrained at Supports**

tw/ts ratio	Analysis Method Type	Natural Frequency ( $\omega$ ) in ( Hz )				
		Mode No. (Single-Cell, Fully Restrained at Supports)				
		1	2	3	4	5
0.5	FEM	7.709	9.051	10.013	11.630	13.026
	PEM	7.78	9.13	10.53	13.53	14.50
1	FEM	12.738	13.818	13.970	15.272	15.856
	PEM	12.83	13.85	14.93	16.33	17.99
1.5	FEM	14.790	15.326	17.989	18.988	19.277
	PEM	14.87	15.50	18.24	20.30	21.62
2	FEM	16.119	17.231	18.820	21.124	22.677
	PEM	16.16	17.30	18.87	22.29	24.04

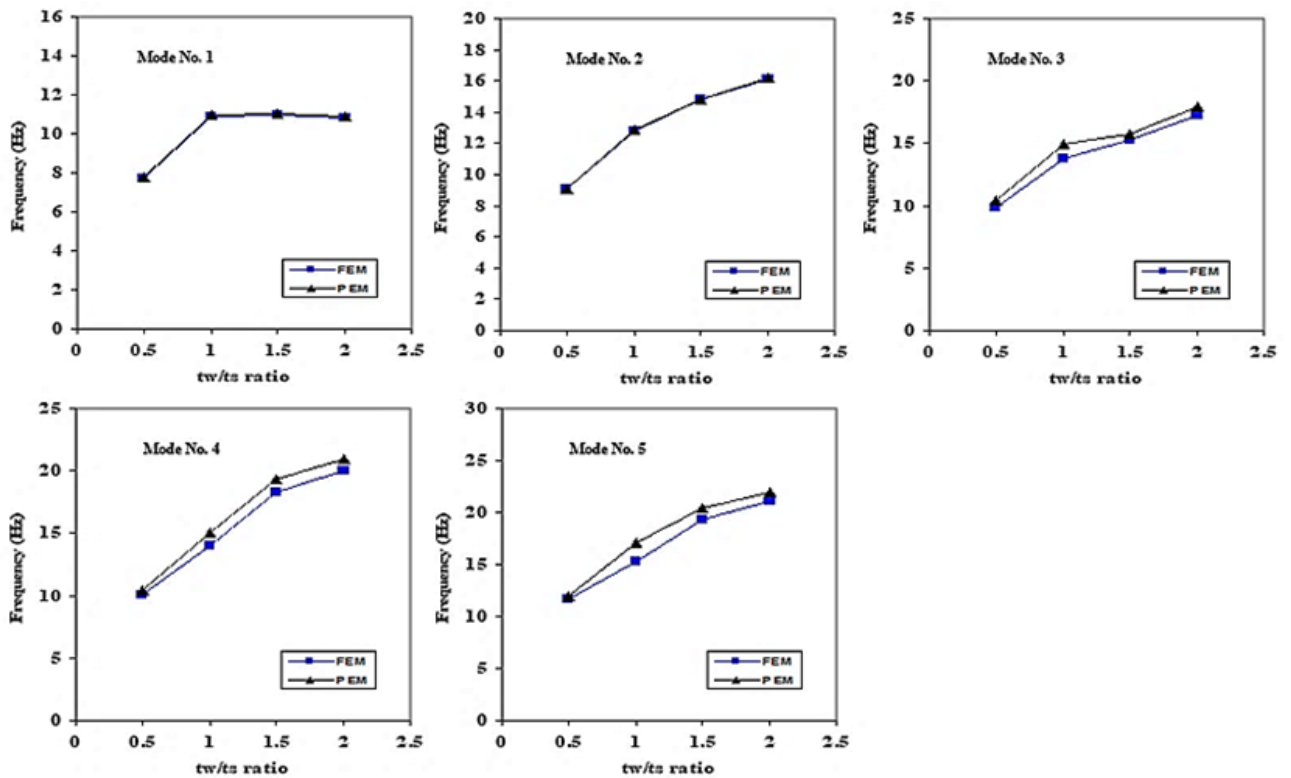


**Fig. 13 - Natural Frequencies vs. (tw/ts) Ratio for a Single Cell Curved Bridge Deck (Partially Restrained)**

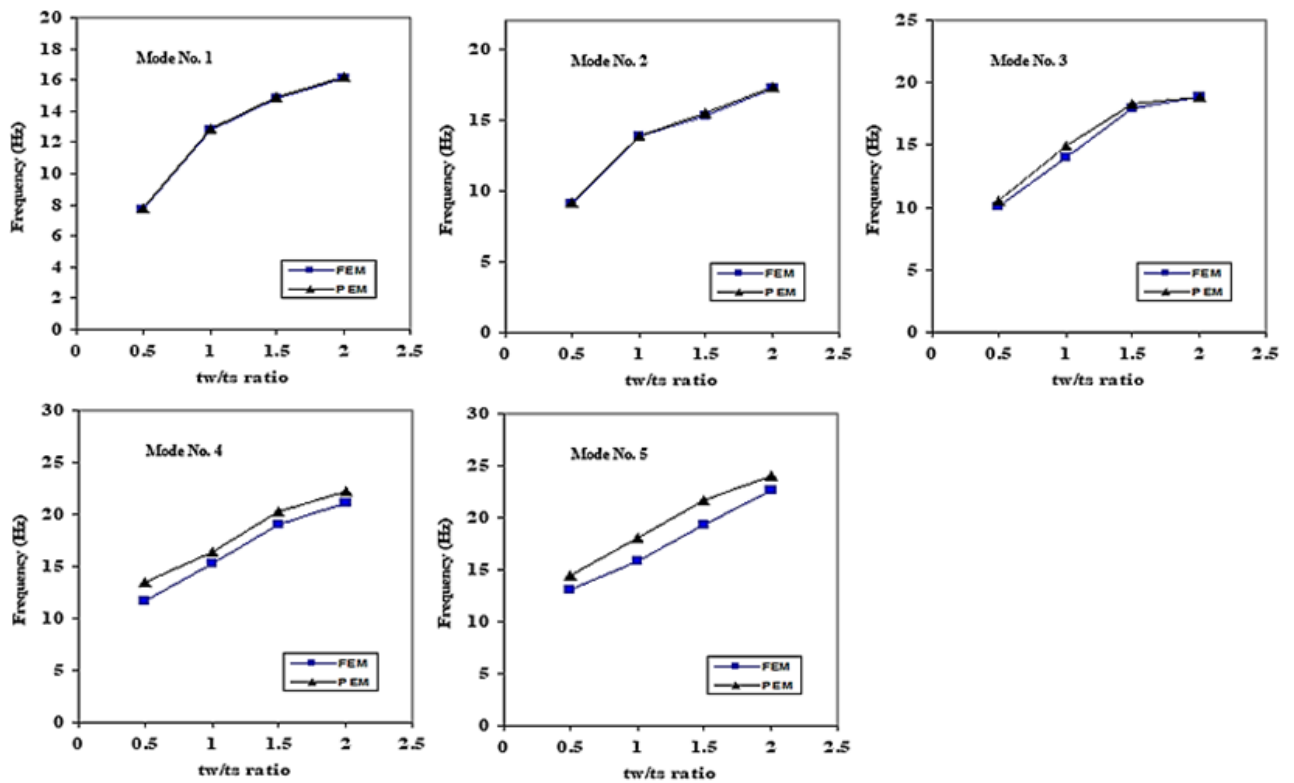


**Fig. 14 - Natural Frequencies vs. (tw/ts) Ratio for a Single Cell Curved Bridge Deck (Fully Restrained)**

### 3.2.3 Effect of Number of Diaphragms

The number of diaphragms corresponds to the number of panels, each being a segment between two diaphragms. Panels range from 2 to 10 to show how diaphragm variation affects free vibration for a constant span. Natural frequencies from the panel element (PE) method are in (Table 9) and (Table 10), with plots in (Fig. 15) and (Fig. 16) for partially and fully restrained supports. The study shows the PE method accurately predicts vibration characteristics as the number of diaphragms increases.

**Table 9. Natural Frequencies vs No. of Diaphragms of a Single-Cell Deck Bridge (Partially Restrained)**

No. of Panels	Analysis Method Type	Natural Frequency ( $\omega$ ) in ( Hz )				
		Mode No. (Single-Cell, Partially Restrained at Supports)				
		1	2	3	4	5
2	FEM	5.467	6.598	6.686	7.025	10.394
	PEM	5.51	6.62	7.36	8.58	12.16
4	FEM	10.957	19.185	20.635	20.917	21.540
	PEM	11.03	19.24	21.13	22.43	23.68
6	FEM	10.455	20.428	29.067	36.361	40.782
	PEM	10.49	20.57	30.01	37.21	42.01
10	FEM	10.256	19.872	28.580	37.965	42.269
	PEM	10.27	20.00	30.60	39.83	45.41

**Table 10. Natural Frequencies vs No. of Diaphragms of a Single-Cell Deck Bridge (Fully Restrained)**

No. of Panels	Analysis Method Type	Natural Frequency ( $\omega$ ) in ( Hz )				
		Mode No. (Single-Cell, Fully Restrained at Supports)				
		1	2	3	4	5
2	FEM	5.485	6.604	6.734	7.688	10.715
	PEM	5.55	6.64	7.02	8.97	11.76
4	FEM	18.239	19.417	20.831	21.025	23.075
	PEM	18.31	19.46	21.87	23.02	25.64



6	FEM	17.160	24.600	36.756	40.641	40.857
	PEM	17.20	24.63	38.08	42.50	41.22
10	FEM	16.674	24.003	38.288	39.851	47.419
	PEM	16.62	24.05	39.19	41.95	49.68

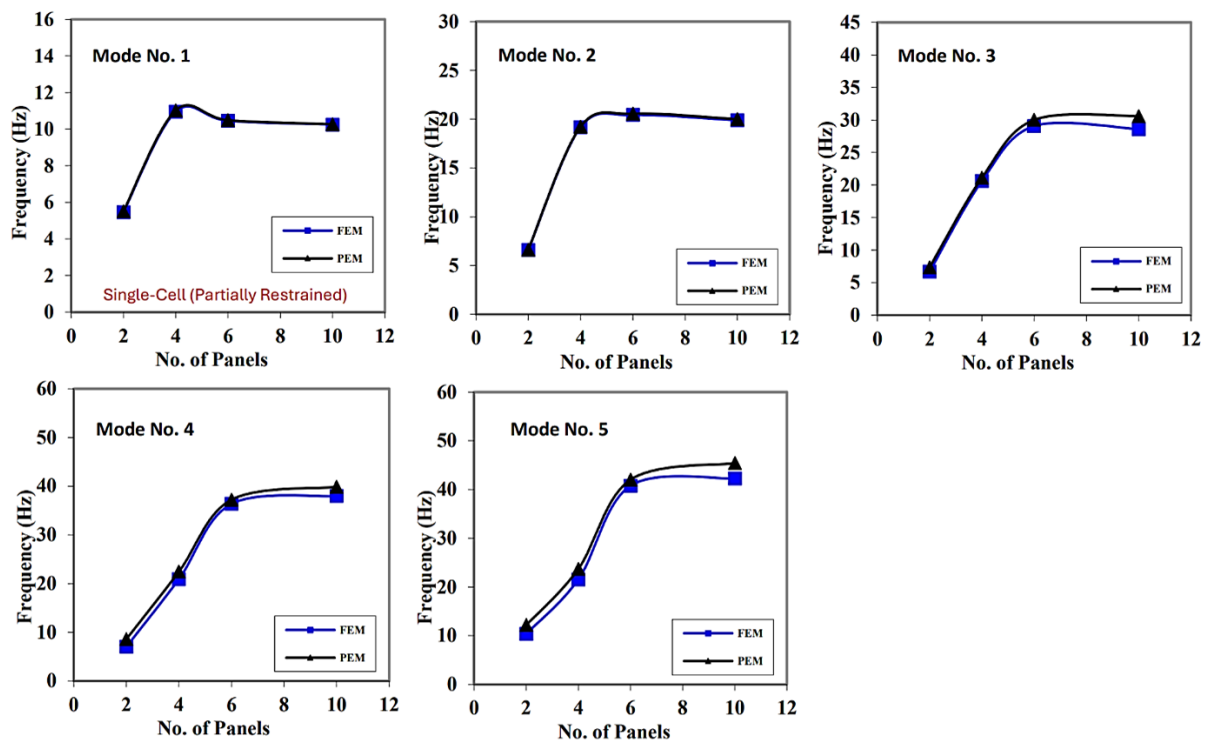


Fig. 15 - Natural Frequencies vs No. of Diaphragms of a Single-Cell Deck Bridge (Partially Restrained).

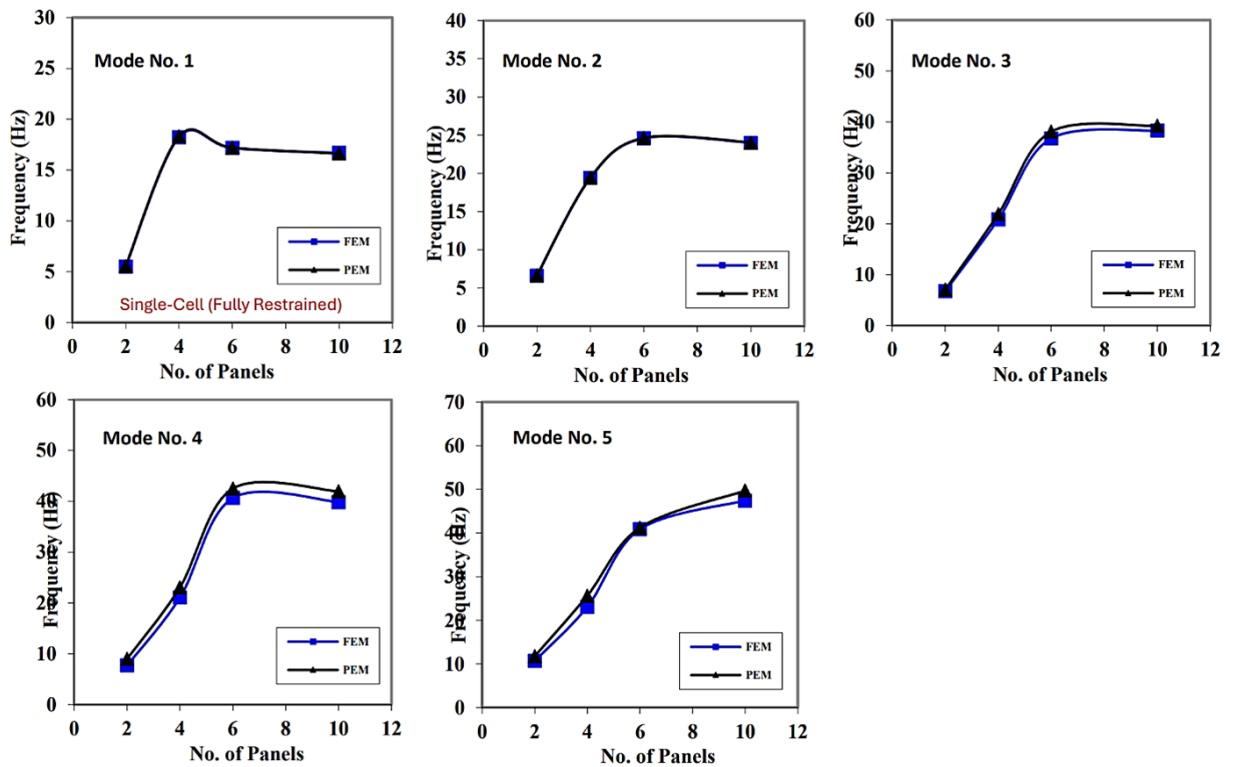


Fig. 16 - Natural Frequencies vs No. of Diaphragms of a Single-Cell Deck Bridge (Fully Restrained)



### 3.2.4 Effect of Live Load

To assess the effect of live load, simple load cases were considered per Iraq's Specifications for Bridge Loading [30]:

1. Lane Loading: Uniformly distributed loads over the deck with a knife-edge load at mid-span for maximum response, designated as load case I.
2. Military Loading: Two classes studied:
  - a) Class 100 (Tracked): One tracked load at mid-span, designated as load case II.
  - b) Class 100 (Wheeled), One wheeled load at mid-span, designated as load case III.

The resulting natural frequencies are listed in (Table 11) and (Table 12) respectively. The proposed Panel Element Method (PEM) showed good agreement with results from the finite element (FE) approach.

**Table 11. Natural Frequencies of Single-Cell Deck Bridge Under Various Live Loads (Partially Restrained)**

Load Case No.	Analysis Method Type	Natural Frequency ( $\omega$ ) in ( Hz )				
		Mode No. (Single-Cell, Partially Restrained at Supports)				
		1	2	3	4	5
I	FEM	10.800	18.910	20.339	20.616	21.231
	PEM	10.85	18.96	20.87	22.91	26.04
II	FEM	10.609	18.576	19.980	20.252	20.856
	PEM	10.58	18.62	21.21	22.12	22.99
III	FEM	10.543	18.461	19.856	20.127	20.727
	PEM	10.60	18.50	25.92	22.02	23.71

**Table 12. Natural Frequencies of Single-Cell Deck Bridge Under Various Live Loads (Fully Restrained)**

Load Case No.	Analysis Method Type	Natural Frequency ( $\omega$ ) in ( Hz )				
		Mode No. (Single-Cell, Fully Restrained at Supports)				
		1	2	3	4	5
I	FEM	17.977	19.138	20.532	20.723	22.744
	PEM	18.04	19.19	21.74	21.97	25.17
II	FEM	17.660	18.800	20.169	20.357	22.342
	PEM	17.68	18.73	22.02	23.29	24.40
III	FEM	17.551	18.684	20.044	20.231	22.204
	PEM	17.59	18.73	23.15	22.20	25.61

The numerical case studies concluded that the developed panel element (PE) approach is a versatile method for evaluating the free vibration characteristics of curved bridge decks with single and double cells across various span lengths and support conditions. While the finite element (FE) approach is reliable, the panel element (PE) method offers significant economic advantages, achieving over 90% reduction in degrees of freedom. This substantial decrease in equations, with only a minor sacrifice in accuracy for the first few vibration modes, is a key outcome of the developed technique.

## 4 Conclusions

Different configurations of curved cellular bridge decks were analyzed to validate the proposed Panel Element Method (PEM) against the Finite Element Method (FEM) for free and forced vibration analysis. Key conclusions from the case studies include:

1. The Panel Element Method (PEM) is a valid and effective approach for the free vibration analysis of curved cellular bridges.
2. Panel Element Method (PEM) accurately predicts the free vibration characteristics (natural frequencies and mode shapes) of single-cell curved box-girder bridge decks, with a difference of less than 7% compared to the Finite Element Method (FEM).
3. The PEM significantly reduces computational effort, achieving over 90% reduction in degrees of freedom compared to traditional FEM.



4. The analysis reveals that partially restrained supports yield lower natural frequencies than fully restrained supports.
5. Increasing the web-to-flange thickness ratio enhances natural frequencies due to improved stiffness.
6. The effect of live loads on natural frequencies was also significant, with variations observed depending on the type of loading applied (lane loading vs. military loading).
7. The limited degrees of freedom required by the PEM significantly reduce the number of equations and iterations, resulting in less error.

## 5 Conflict of Interests

The authors declare no conflict of interest.

### References

- 1 Mohammed, H.H., Naser, A.F., Qin, L.H. (2024). Appearance inspection and finite element analysis of posttension concrete horizontal curved box girder bridge: Static and dynamic analysis. *Mathematical Modelling of Engineering Problems*, **11(10)**, 2606-2614. <https://doi.org/10.18280/mmep.111002>
- 2 Huffington, Jr. N. J. and Hoppmann, II. W. H. (2021). On the Transverse Vibrations of Rectangular Orthotropic Plates. *ASME. J. Appl. Mech.* Sep 1958, **25(3)**, 389-395. <https://doi.org/10.1115/1.4011833>
- 3 Cheung, M. S., Cheung, Y. K., & Reddy, D. V. (1971). Frequency Analysis of Certain Single and Continuous Span Bridges. *Development in Bridge Design and Construction*, 188-199. <https://trid.trb.org/View/100039>
- 4 Bickford, W. B., & Strom, B. T. (1975). Vibration of plane curved beams. *Journal of Sound and Vibration*, **39(2)**, 135-146. [https://doi.org/10.1016/s0022-460x\(75\)80213-6](https://doi.org/10.1016/s0022-460x(75)80213-6)
- 5 Al-Khazraji, Shatha Mohammed & Ali, Adnan. (2010). Structural Idealization for Free Vibration of Curved Cellular Bridge Decks. *The 2nd Regional Conference for Engineering Sciences*, College of Engineering, Al Nahrain University, Baghdad, Iraq, **1(6)**. [https://www.researchgate.net/publication/338630916\\_Structural\\_Idealization\\_for\\_Free\\_Vibration\\_of\\_Curved\\_Cellular\\_Bridge\\_Decks](https://www.researchgate.net/publication/338630916_Structural_Idealization_for_Free_Vibration_of_Curved_Cellular_Bridge_Decks)
- 6 Agarwal, P., Pal, P., Mehta, P.K. (2022). Free Vibration Analysis of RC Box-Girder Bridges Using FEM. *Sound & Vibration*, **56(2)**, 105–125. <https://doi.org/10.32604/sv.2022.014874>
- 7 Nidhi Gupta, Preeti Agarwal, & Priyaranjan Pal. (2019). Free Vibration Analysis of RCC Curved Box Girder Bridges. *International Journal of Technical Innovation in Modern Engineering & Science (IJTIMES)*, ICMTCE-2019 (International Conference on Modern Trends in Civil Engineering -Towards Sustainable Development Goals), **5(13)**, 1-7. <https://ijtimes.com/index.php/ijtimes/article/view/3001>
- 8 Verma, V., & Nallasivam, K. (2023). Dynamic interaction analysis of a high-speed train vehicle and a thin-walled curved box-girder bridge with a sub-track system by finite element method. *Asian Journal of Civil Engineering*, **24**, 3437–3462. <https://doi.org/10.1007/s42107-023-00724-z>
- 9 Xiang, P., Yan, W., Li-Jiang, Wang-Zhou, Wei, B., & Liu, X. (2023). Resonance analysis of a high-speed railway bridge using a stochastic finite element method. *Earthquake Engineering and Engineering Vibration*, **22**, 1015–1030. <https://doi.org/10.1007/s11803-023-2217-5>
- 10 Zhu, C., Li, W., & Wang, H. (2023). Analysis of Interlayer Crack Propagation and Strength Prediction of Steel Bridge Deck Asphalt Pavement Based on Extended Finite Element Method and Cohesive Zone Model (XFEM–CZM) Coupling. *Coatings*, **13(11)**, 1973. <https://doi.org/10.3390/coatings13111973>
- 11 Ahmad, A., Ahmed, A., Iqbal, M., Ali, S. M., Khan, G., Eldin, S. M., & Yosri, A. M. (2023). Non-linear finite element modeling of damages in bridge piers subjected to lateral monotonic loading. *Scientific Reports*, **13(1)**, 13461. <https://doi.org/10.1038/s41598-023-39577-6>
- 12 Yang, X. (2024). Mechanical Analysis and Optimization of Concrete Structures Based on Advanced Finite Element Method. *European Journal of Computational Mechanics*, 507-534. <https://doi.org/10.13052/ejcm2642-2085.3354>
- 13 Wang, F. (2024). Research on dynamic detection method of bridge vehicle load based on optimization algorithm. *Applied Mathematics and Nonlinear Sciences*, **9(1)**, 4.

Temimi, F.A.A.; Ahmed, A.R.; Obaidi, A.H.F.; Yermoshin, N.

Vibration characteristics of 3D curved cellular bridges via panel element method

2025; Construction of Unique Buildings and Structures; **116** Article No 11601. doi: 10.4123/CUBS.116.1



- <https://doi.org/10.2478/amns.2023.2.00028>
- 14 Rachid, A., Ouinas, D., Lousdad, A., Zaoui, F. Z., Achour, B., Gasmi, H., Butt, T., & Tounsi, A. (2022). Mechanical behavior and free vibration analysis of FG doubly curved shells on elastic foundation via a new modified displacements field model of 2D and quasi-3D HSDTs. *Thin-walled structures*. <https://doi.org/10.1016/j.tws.2022.107123>
  - 15 Wei, G., Lardeur, P., & Druesne, F. (2023). Free vibration analysis of thin to thick straight or curved beams by a solid-3D beam finite element method. *Thin-walled structures*. <https://doi.org/10.1016/j.tws.2023.107123>
  - 16 Wodzinowski, R. A. (2021). Free Vibration Analysis of Horizontally Curved Composite Concrete Deck Over Steel I-Girder Bridges. *Proceedings of the International Conference on Structural Engineering*. <https://doi.org/10.1007/s12345-021-01234-5>
  - 17 Al\_Temimi, Feras A. R. (2014). Earthquake Analysis of Curved Cellular Bridges. *Iraqi digital Repository*, University of Baghdad, College of Engineering, Department of Civil Engineering. <https://iqdr.iq/search?view=ba8ceedaf306b2202de35a490bd16878>
  - 18 Ayubirad, M. S., Ataei, S., & Tajali, M. (2024). Numerical Model Updating and Validation of a Truss Railway Bridge considering Train-Track-Bridge Interaction Dynamics. *Shock and Vibration*, **2024(1)**, 4469500. <https://doi.org/10.1155/2024%2F4469500>
  - 19 Gomez, D., Dyke, S. J., & Rietdyk, S. (2018). Experimental Verification of a Substructure-Based Model to Describe Pedestrian–Bridge Interaction. *Journal of Bridge Engineering*, **23(4)**, 04018013. <https://doi.org/10.1061/%28ASCE%29BE.1943-5592.0001204>
  - 20 Verma, V., Wani, K. U. F., & Dhiman, S. (2025). A study on factors influencing dynamic response of thin-walled box-girder railway bridge subjected to high-speed train load through regression modeling. *World Journal of Engineering*. <https://doi.org/10.1108/wje-07-2024-0414>
  - 21 Zhang, X., Ruan, L.-Y., Zhao, Y., Zhou, X., & Li, X. (2020). A frequency domain model for analysing vibrations in large-scale integrated building–bridge structures induced by running trains. *Proceedings of the Institution of Mechanical Engineers, Part F, Journal of Rail and Rapid Transit*, **234**, 226–241. <https://doi.org/10.1177/0954409719841793>
  - 22 Consolazio, G., Hendrix, J. L., McVay, M., Williams, M., & Bollmann, H. (2004). Prediction of Pier Response to Barge Impacts with Design-Oriented Dynamic Finite Element Analysis. *Transportation Research Record*, **1868**, 177–189. <https://doi.org/10.3141/1868-19>
  - 23 Owerko, P. (2018). The stochastic finite element method in the assessment of bridge infrastructure objects-review. *E3S Web of Conferences*, EDP Sciences, **45**, 00062. <https://doi.org/10.1051/E3SCONF%2F20184500062>
  - 24 Micelli, F., Maci, L., & De Vitis, F. A. (2023). Buckling analysis of steel members by extension of EC-3 methods in bridge girders under Patch Loading. *ce/papers*, **6(5)**, 79-88. <https://doi.org/10.1002/cepa.2178>
  - 25 Robert D. Cook, David S. Malkus, Michael E. Plesha, Robert J. Witt. (2002). Concepts and Applications of Finite Element Analysis, *John Wiley and Sons*, New York (N.Y.), 4th ed. <https://lib.ugent.be/catalog/rug01:001798729>
  - 26 Kaveh, A. (Ali). (2004). Structural Mechanics: Graph and Matrix Methods. *Computational Structures Technology Series*, Research Studies Press Ltd (John Wiley). Exeter. U.K. 3rd ed. [https://search.library.berkeley.edu/permalink/01UCS\\_BER/1thfj9n/alma991044261299706532](https://search.library.berkeley.edu/permalink/01UCS_BER/1thfj9n/alma991044261299706532)
  - 27 Krishnamoorthy C. S. (2019). Finite Element Analysis: Theory and Programming. *Mcgrawhill*. 2nd ed. <https://www.amazon.com/Finite-Element-Analysis-Theory-Programming/dp/0074622102>
  - 28 Clough, Ray W., Joseph Penzien. (2003). Dynamics of Structures. *Computers & Structures, Inc.*, 3rd ed. <http://parastesh.usc.ac.ir/files/1538888752479.pdf>
  - 29 Paz M., Kim Y. H. (2019). Structural Dynamics: Theory and Computation. *Springer Cham*. New York. 6th ed. <https://doi.org/10.1007/978-3-319-94743-3>
  - 30 Iraqi Standard Specifications for Road Bridges. (1987). Loadings. *Ministry of Housing & Construction*, State Organization of Roads and Bridges, Baghdad. Revised Edition. <https://www.scribd.com/document/712916832/Iraq-Standard-Specifications-For>